Int J Adv Manuf Technol (2011) 53:1063–1073
DOI 10.1007/s00170-010-2893-y

ORIGINAL ARTICLE

An experimental approach to study the capability of end-milling for microcutting of glass

Muhammad Arif · Mustafizur Rahman · Wong Yoke San · Neha Doshi

Received: 29 April 2010 / Accepted: 8 August 2010 / Published online: 24 August 2010

Abstract Glass is a hard and brittle material. It is finding mounting quantum of applications in semiconductor, opto-electronics, and mold manufacturing sectors. However, glass is not amenable to machining because of its low fracture toughness. If machined with conventional approach, the mechanism of material removal in machining of glass is fracture based that results into poor quality of the machined surface and imparts subsurface damage. In order to achieve superior surface finish, glass must be machined in ductile mode. Ductile-mode machining is now a well-established technique but most of the work has been performed with single-point cutting processes. To assess the capability of ductile-mode machining with multipoint cutting process, fundamental studies are highly desired. This paper reports the results of an experimental investigation into ductile-mode machining of glass by milling process. Side-milling tests have been performed on the glass workpiece to identify the key parameters governing the ductile-brittle transition mechanism. Experimental results demonstrate that fracture-free surface can be machined on glass by milling process. Cutting forces were analyzed to comprehend the dynamic behavior of the cutting process in ductile mode.

Keywords Ductile machining · Glass machining · End-milling · Precision machining

1 Introduction

Glass is a hard and brittle material. Glass has amorphous structure and atoms are present in the structure in randomized arrangement forming longer chains. The high brittleness of glass is due to its amorphous structure. Since atoms do not form planes that can slip past each other, stress relieving cannot occur. Excessive stress forms a crack that grows in size under loading and eventually causes the glass to undergo cleavage or brittle fracture. Notwithstanding, optical glasses have some excellent mechanical and physical properties such as high hardness, optical transparency, various refractive indices, homogeneity, isotropy, good corrosion and chemical resistance, and high electrical resistivity [1, 2]. This makes glass a versatile engineering material. It is widely used in automotive, communications, optics, electronics, architectural, and biomedical industries [3]. There are many types of glass depending upon its chemical composition. Soda-lime glass is the most prevalent type of commercial glass. Soda-lime glass is prepared by melting and mixing silica with soda, dolomite, lime and alumina at a temperature of up to 1,675°C [4]. Typical applications of soda-lime glass include mirrors, microscopic slides, touch screens, filters, photo masks, glass masters, data storage disks, printed circuit substrates, photographic plates, wafers, and optical windows (http://www.valleydesign.com/sodalime.htm. Accessed 10 March 2010). It is highly desirable to obtain nanometric surface finish on optical glasses owing to the advantage of improved performance of the components [5]. However, glass is not amenable to machining with conventional approach due to its low fracture toughness. Traditionally, a shape on the glass is made by grinding or abrasive based process that imparts surface and subsurface damage. The damage caused by the grinding is then removed by polishing to obtain mirror like surface finish with less than 20 nm R_{max} on the machined surface [1, 2]. Polishing process is extremely slow and time consuming [1]. Ductile-mode machining has the potential to replace slow

M. Arif (✉) · M. Rahman · W. Y. San · N. Doshi
National University of Singapore,
Kent Ridge, Singapore
e-mail: arif@nus.edu.sg
URL: www.me.nus.edu.sg

polishing and abrasive based finishing processes [6]. According to the hypothesis of ductile machining, all materials, regardless of their hardness and brittleness, will undergo a transition from brittle to ductile machining regime below a critical undeformed chip thickness. Below this threshold, the energy required to propagate cracks is believed to be larger than the energy required for plastic deformation, so that plastic deformation is the predominant mechanism of material removal in machining these materials [5]. This hypothesis came from indentation tests performed on glass where a plastic deformation zone was observed to have been produced before cracks could be initiated at a critical load [7]. The feasibility of ductile mode with single-point diamond turning has been reported in earlier literature [8–16]. It was established [17] that the presence of hydrostatic compressive force was necessary to suppress the crack propagation in the cutting zone. This condition can only be obtained if the stress field is very small that corresponds to submicron values of undeformed chip thickness or depth of cut [18]. In order to achieve ductile-mode machining of brittle materials in single-point turning, a high-precision turning machine is a basic requirement. The machine tool must be stiff enough to provide extremely high tool position accuracy in the nanometer range [19]. When the feed rate or depth of cut exceeds a critical value, the mechanism of material removal in brittle workpiece changes from defined ductile to undefined brittle, with several different crack systems [20–22]. Furthermore, single-point turning causes some machining troubles like chatter vibration, tool chipping and faster tool wear. The material removal rate is also not high enough due to extremely small feeds and depth of cuts. In addition to these stringent constraints, single-point turning cannot produce asymmetrical features on the workpiece. With rapid development in microelectronics, the demand for microcomponents having complex geometries is on rise. With application of hard materials in more diversified products like molds and dies for injection molding of consumer products, complicated features and cavities are required to be produced in the brittle work material. End-milling process is capable to produce three-dimensional (3D) features and free forms on workpiece. Major problems for micro-milling are unpredictable cutting tool life and premature tool failure [23]. Tool condition monitoring is therefore very important aspect in micro-milling to improve productivity of the process by minimizing non-productive time due to timely detection of tool failure. Tool condition can be monitored by direct or indirect methods. Direct method involves optical sensing and indirect method is based on measurement of several operational parameters such as cutting forces, acoustic emission, and tool vibrations [23, 24]. Stavropoulos et al. [25] presented a combinational method based on vibration and acoustic emission caused by the micro-milling process for developing a process monitoring system that is capable of monitoring simultaneously the spindle's and tool's condition during micro-milling operations. With proper tool condition monitoring systems installed, micro-milling can also be successfully performed with microsize diameter cutters to create miniaturized feature on brittle materials. Such miniaturized features are otherwise difficult to machine with desired accuracy by non-conventional processes like chemical etching and ultrasonic vibration machining due to non-deterministic nature of the material removal. With extensive literature available on ductile machining based on single-point tool, studies on ductile machining with multipoint cutting tool have not been made to a sufficient extent. Takeuchi and Sata [26] performed ultraprecision 3D micromachining of glass workpiece by means of a lathe-type ultraprecision-milling machine and pseudo ball end-mills. They obtained glass mask of 1 mm in diameter with the surface roughness of 50 nm. Matsumura [3, 27–30] performed milling of glass in ductile mode by using flat and ball end-mills. He machined microchannels in glass by using carbide ball end-mill. These studies have exhibited decent promise for achieving fracture-free three-dimensional features on glass. The fundamental studies are still needed to better understand the mechanism of ductile-mode machining of brittle materials by milling process. One of the most critical issues in ductile mode machining has been the high cost of diamond tool due to excessive wear. In our work, a wide range of cutting conditions has been used to study the ductile-mode machining of soda-lime glass. The study identifies the influence of two cardinal cutting parameters on the occurrence of ductile-mode machining. Furthermore, carbide end-mill has been used for machining of glass. With the development of nano-scale grain size, it has become possible to make super hard cemented carbide end-mills with sharp cutting edge [27, 29, 30]. To the best of the authors' knowledge, this is the first study that has used cemented carbide flat end-mill to achieve ductile-mode machining of glass. The tool wear study has also been conducted to identify the wear pattern of the end-mill. The study is expected to make significant contribution to the current state of research in ultraprecision machining of brittle materials.

2 Mechanism of microcutting by end-milling

Mechanics of milling is more complex than single edge processes. There are two cutting operations for an end-milling operation, side-milling and slot-milling. Furthermore, side-milling has two strategies of cutting namely up-milling and down-milling. This study has used up-milling approach. In up-

milling, the uncut chip thickness starts from minimum value at the beginning of cut or engagement of cutter with workpiece and approaches to a higher value as the cutter rotates. It reaches the maximum possible value for a specific radial depth of cut and feed per edge at the end of the cut or just before the cutter disengages from the workpiece. According to the condition of ductile machining, there exists a critical value of undeformed chip thickness for ductile-brittle transition. The ductile-mode machining is possible below this critical value of uncut chip thickness and mode of machining is transitioned into brittle one as soon as the uncut chip thickness exceeds the critical value. So at the beginning of cut in up-milling, there is possibility of achieving ductile machining at small values of uncut chip thickness. There is also minimum chip thickness effect in milling because the value of uncut chip thickness at the beginning of the cut is too small to be removed by the cutting edge in each pass [31–33]. This results into plowing or elastic deformation. Since uncut chip thickness is increased from zero to maximum in milling, the material is only rubbed until minimum chip thickness is reached. The rubbing or plowing adds to the surface roughness of the workpiece. As the cutter continues to rotate, the uncut chip thickness increases and exceeds minimum uncut chip thickness required for cutting action to take place effectively. This is the zone of ductile-mode machining. Depending upon feed per edge and radial depth of cut, if the increasing value of uncut chip thickness reaches the critical value for ductile-brittle transition at a certain angle of cutter rotation before the cutter disengages from the workpiece, brittle fracture will take place. Now if the point of occurrence of brittle fracture is sufficiently far away from the level of final machined surface, the fractured region will be removed by the cutting action of the subsequent edge Fig. 1. The final machined surface, in this case, will be fracture free.

However, if the occurrence of brittle fracture is too close to the level of final machined surface, the size of fracture allows it to reach below the level of final machined surface. In this case, the subsequent cutting edge cannot remove the fractured zone and this fracture will sustain on the final machined surface resulting into a brittle mode machined as shown in Fig. 2. Therefore, controlling the location of fracture point is the key in milling process.

The point of occurrence of brittle fracture is controlled by the feed per edge. However, whether that point will be reached practically, in a specific cut, also depends upon the radial depth of cut. A finer value of feed per edge will delay the occurrence of brittle fracture allowing the subsequent cut to remove the fracture affected zone. On the other hand, a higher value of feed per edge causes the fracture to occur too early resulting into brittle mode machined surface. Likewise, with feed per edge being constant, the maximum value of uncut chip thickness achieved in a cut is larger for higher radial depth (Fig. 3b) of cut compared with that at smaller radial depth of cut (Fig. 3a).

In milling, chip thickness $\boldsymbol{h}$ can be given by following relation:

$$h = f_e \sin\theta \text{ if } f_e << R$$

Where $\boldsymbol{f_e}$ is feed per edge, R is radius of the cutter, and $\boldsymbol{\theta}$ is rotation angle of the cutter in the cut (Fig. 4).

In ductile-mode milling, if a higher value of feed per edge is used, $\boldsymbol{\theta}$ decreases for constant value of critical chip thickness. It means fracture occurs very close to the final machined surface. It is, therefore, important to mention here that effectively the critical feed per edge in the end-milling process is not the one at which ductile-brittle transition occurs but the one that gives sufficiently large $\boldsymbol{\theta}$ so that fracture point could remain far from final machined surface for high radial depth of cut.

The phenomenon of removal of fracture affected zone by the subsequent cutting edge in milling process offers great advantage over the single edge cutting process. In single-edge cutting process, if the fracture occurs due to exceeding critical

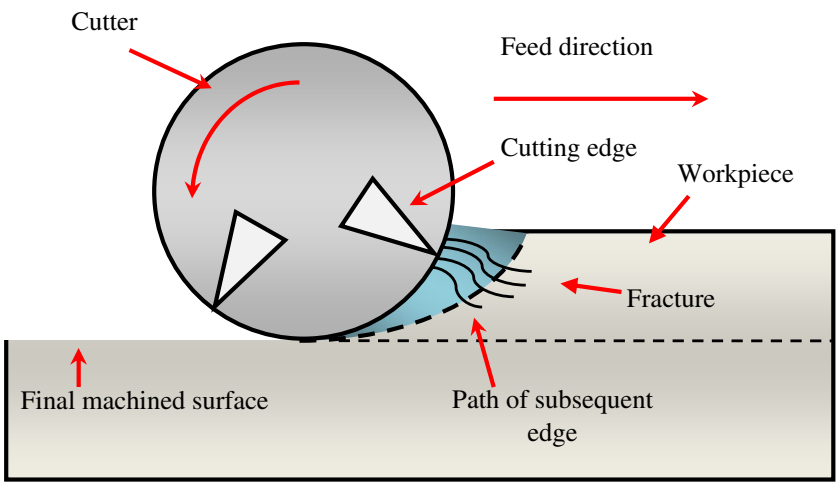

Fig. 1 End-milling process at small feed rate

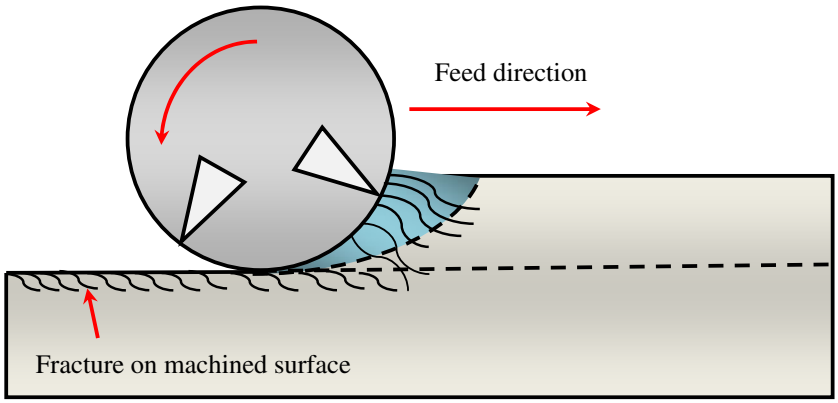

Fig. 2 End-milling process at high feed rate

value of depth of cut, there is no subsequent edge to remove the fractured portion resulting into brittle mode machining Fig. 5.

For sufficiently high feed per edge, there are three possible effects that can occur in milling process; plowing at the beginning of cut, ductile-mode machining beyond the plowing zone and brittle fracture zone for uncut chip thickness values beyond the critical value for ductile-brittle transition [27, 30]. If the fracture is prevented from reaching the final machined surface, such machined surface obtained by side cutting still has somewhat non-uniform

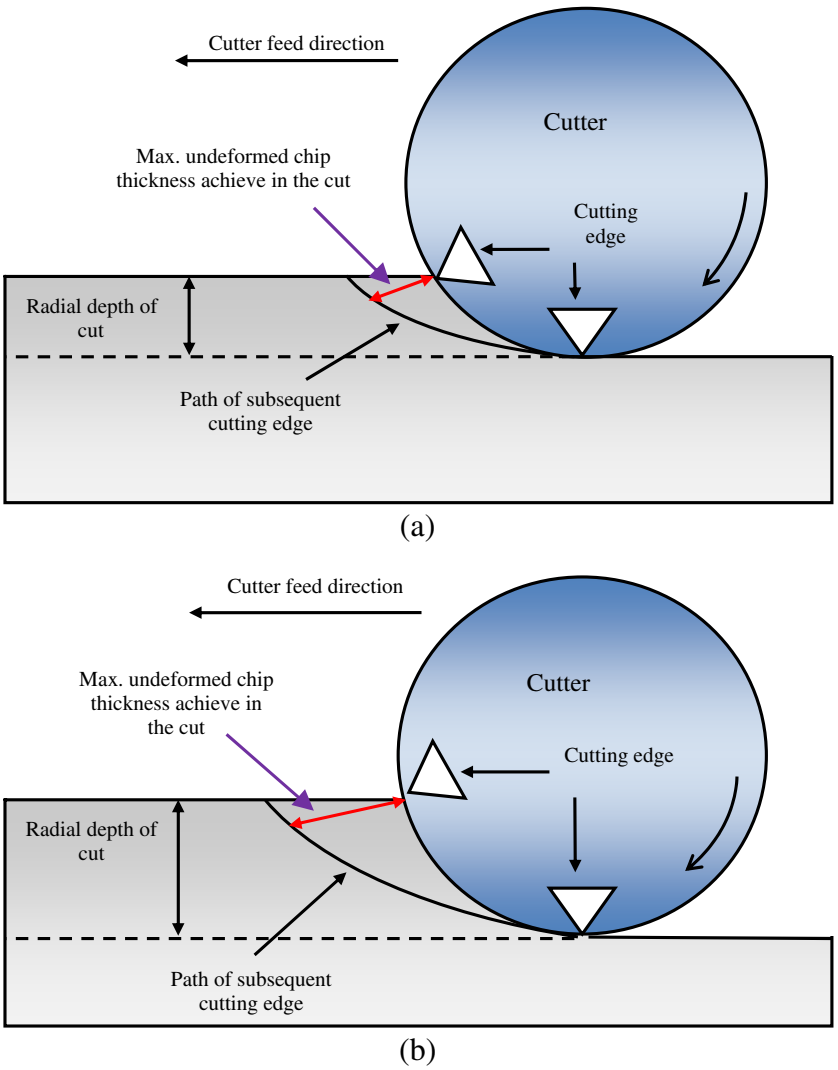

Fig. 3 Maximum uncut chip thickness achieved at constant feed per edge and at **a** small radial depth of cut and **b** at higher radial depth of cut in end-milling

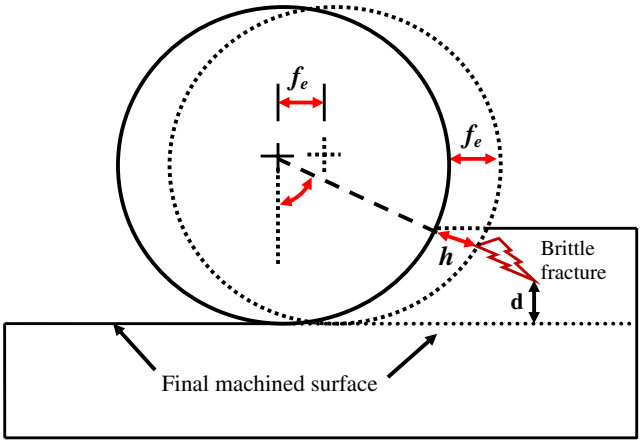

Fig. 4 Geometry of end-milling (for same critical chip thickness h, as f_e increases, θ decreases and d also decreases, so brittle fracture moves closer to the final machined surface)

surface roughness with few marks of plowing present on it. The average surface roughness achieved in milling is, therefore, expected to be slightly higher than a contemporary single edge process.

After machining, the characterization of machined surface has been demonstrated in various ways. Ductile machining generates a fracture free and smooth surface [15]. Liu [15] observed that continuous chip may not be the only criteria to establish ductile machining as he obtained a very smooth machined surface with relatively shorter chips. The transition has also been determined by the ratio of cutting and thrust

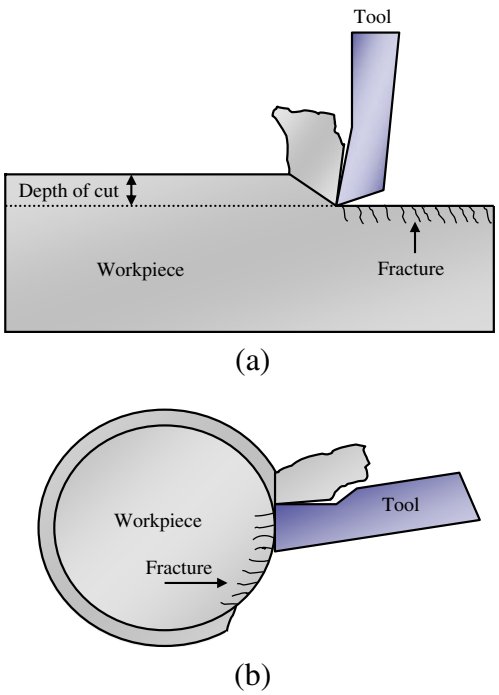

Fig. 5 Single-point machining processes **a** shaping and **b** turning

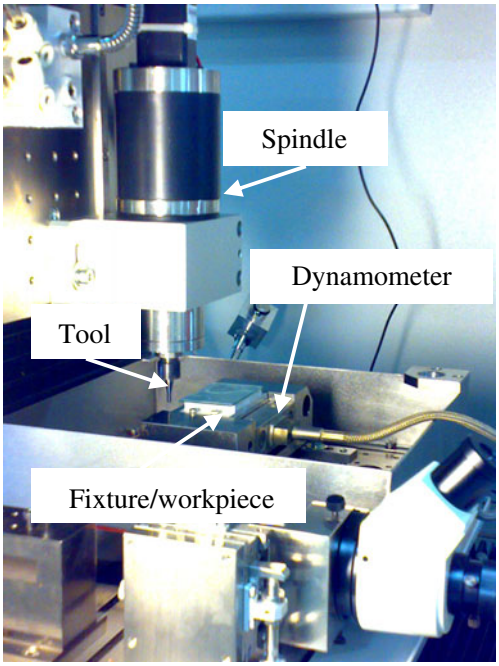

Fig. 6 Vertical spindle miniaturized machine tool

forces [34–37] and the appearance of periodic fluctuation in cutting force signal due to repeated brittle fracture [28]. However study conducted by Matsumura [28] established that though periodic fluctuation was marked in the cutting force signal, the surface was still fracture free due to the removal of damage by the cutting action of the next teeth as discussed earlier. So, even fluctuation in cutting forces may not be the criteria to characterize the state of surface machined by milling process. Surface observation is, therefore, very important consideration in peripheral or side-milling to determine the integrity of machined surface. This study uses side-milling approach to investigate the cutting process by cutting through the entire thickness of the workpiece. This approach enables relatively higher feeds and material removal rate than in slot-milling to machine a surface similar to orthogonal process. Furthermore, it makes the cutting process relatively simple by eliminating the requirement to control the fracture in the axial direction of the cutter.

Table 1 Properties of soda-lime glass

Chemical composition (wt.%)	73SiO2, 14Na2O, 9 CaO, 4 MgO
Glass transition temperature	564°C
Coefficient of thermal expansion	9.5(ppm/K, ~100–300°C)
Density	2.53 g/cm^3 at 20°C
Young's modulus	74 GPa
Shear modulus	29.8 GPa
Fracture toughness	1.0 MPa √m

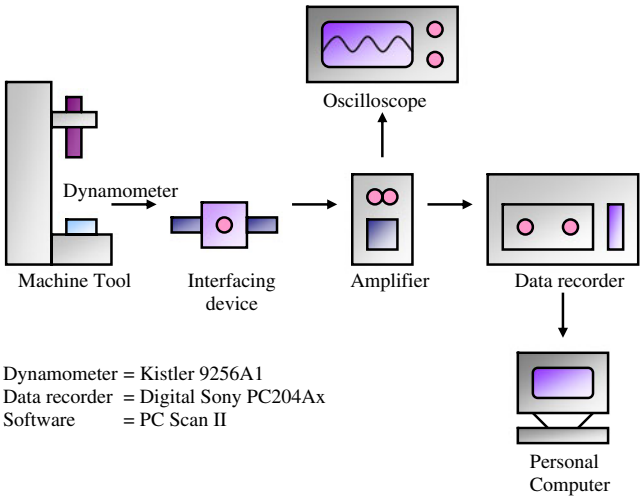

Fig. 7 Experimental setup and control

3 Experimental setup and design

3.1 Machine tool

A 3-axis vertical spindle multipurpose machine tool (Mikrotool DT110) shown in Fig. 6, was used in this experiment. The resolution and positioning accuracy of machine tool motion are at submicron level. The spindle speed is up to 3,000 rpm.

3.2 Cutting tool and workpiece

A 4-flute, TiAlN coated, super fine grain cemented carbide end-mill of 3-mm diameter was used for cutting. The cutting edge radius of the tool used in this study was at submicron scale. A relative higher diameter of the cutter was selected to minimize tool deflection. The helix and rake angles of the tool were 30° and −5°, respectively. The negative rake angle helps to maintain hydrostatic compressive stress in the cutting zone that plays a cardinal role in transition of material behavior from brittle to ductile mode. A new cutter was used for each cut to minimize variation in results due to wear of cutting edge. Rectangular workpieces of soda-lime glass with dimensions of 50×35×1 mm were used in the cutting test. The properties and composition of workpiece material is shown in Table 1. Side-cutting tests have been performed in this study to achieve more controlled cutting action. The side-milling was performed by using up-milling technique.

3.3 Data acquisition

Kistler 9256A1 dynamometer was used to measure the cutting forces generated during machining. The dynamometer measures the forces along feed and crossfeed directions. The forces were subsequently converted into tangential and radial components by using transformation matrix for up-milling. The workpiece was bonded to the fixture by using heat softened glue. The fixture was mounted on dynamometer and dynamometer was fixed on the machine table by using a vacuum chuck. The cutting force signal was connected to data recorder and oscilloscope via an amplifier. The force data was studied using PC Scan II software. A schematic of the experimental setup and control is shown in Fig. 7.

3.4 Zero point setting

The oscilloscope was used to set the datum or zero point after mounting each cutter to minimize the variation in results due to change in setup. The cutter was moved close to the workpiece surface. A magnified lens was used to determine when the cutter was very close to touch the workpiece surface. At that stage the rotating cutter was fed towards the workpiece in submicron level increments. Since workpiece was mounted on a very sensitive dynamometer and dynamometer signal was connected to oscilloscope after passing through an amplifier, a peak was appeared on the oscilloscope screen at the time when cutter just came in contact with the workpiece. That point was set as zero or reference point. This zero setting was mainly required for *y*-axis (crossfeed) to achieve precision in radial depth of cut. The *z*-axis was in axial and *x*-axis was in feed direction of the cutter.

3.5 Selection of cutting parameters

A relatively low cutting speed was (less than 10 m/min) selected to prevent thermal softening of glass due to heat generated in the cutting zone. In this way, heat generated in the cutting zone is thought to have no significant effect on the mode of cutting and it is expected that ductile-mode cutting achieved was due to designated cutting conditions. The cutting conditions used in the experiments are given in the Table 2.

Table 2 Cutting conditions, spindle RPM=1,000, axial depth of cut=1 mm

Test No.	1	2	3	4	5	6	7	8	9	10	11	12	13	14	15	16	17
Radial depth of cut (μm)	2	5	5	20	20	50	50	150	150	200	200	275	350	375	375	400	425
Feed																	
mm/min	25	25	18	18	10	10	6	6	4.5	4.5	4	4	4	4	3.5	3.5	3.5
μm/edge	6.25	6.25	4.5	4.5	2.5	2.5	1.5	1.5	1.12	1.12	1	1	1	1	0.875	0.875	0.875

Table 3 Modes of machining achieved

Test No.	1	2	3	4	5	6	7	8	9	10	11	12	13	14	15	16	17
Achieved mode of machining	D	B	D	B	D	B	D	B	D	PD	D	D	PD	B	D	D	D

D ductile, *B* brittle, *PD* partial ductile

3.6 Surface characterization

After machining, the machined surface was cleaned in acetone by applying ultrasonic vibrations. The machined surface was then observed under optical microscope for surface characterization. The surface topography was examined by atomic force microscope (AFM).

4 Results and discussion

The modes of machining achieved under specified cutting conditions are shown in Table 3.

First side-milling tests were performed with very small radial depth of cut to assess the occurrence of ductile machining and then the radial depth of cut was increased to observe the ductile-brittle transition phenomenon. Different feed rates were applied to investigate the feed rate effect on mode of machining. Fig. 8a shows that there were few marks left on the surface machined at radial depth of cut of 2 μm though the surface was machined in ductile mode. This was due to radial depth of cut being too small to remove grinding marks already present on the workpiece surface before machining. However, a more improved surface was obtained at relatively higher radial depth of cut and as shown in Fig. 8b. Few marks still left on the surface were glass chips adhered to the machined surface but no fracture marks were seen on the machined surface.

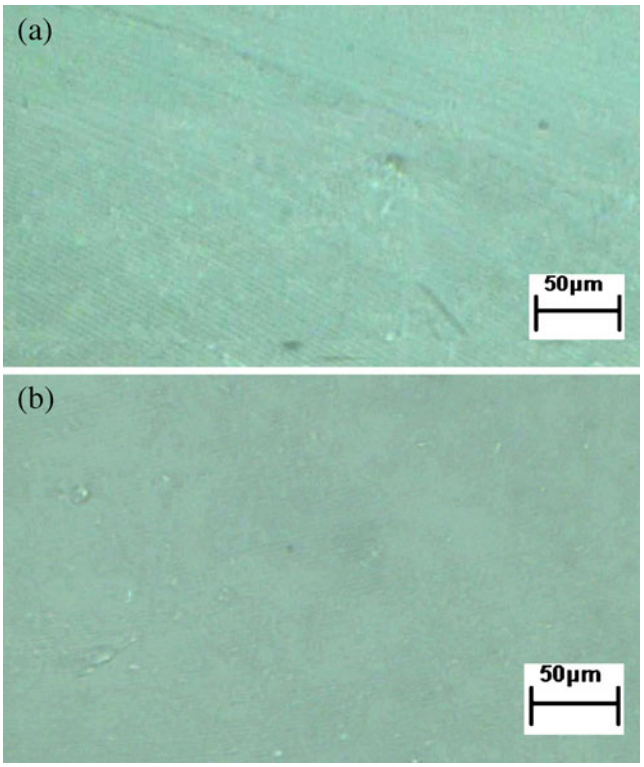

Fig. 8 Images of surfaces machined at **a** radial depth of cut=2 μm, feed rate=25 mm/min, and **b** radial depth of cut=5 μm, feed rate=18 mm/min

The chip adhesion on machined surface is more visible in Fig. 9. This is possibly because dry cutting conditions used in the cutting test and 4-flute cutter geometry do not facilitate the disposal of chips efficiently. High hydrostatic pressure developed under ductile cutting conditions may cause the glass to undergo phase transition and this condition also favors the chips adhesion to the machined surface.

Brittle fracture occurred at high feed rate even at reasonably smaller depth of cut as shown in Fig. 10a. This indicates that at this cutting condition the point of brittle fracture was not adequately far from the level of machined surface and fracture damage penetrated into the machined surface. The experimental results also indicate that fracture-free surface was obtained at high radial depth of cut with feed rate being sufficiently small as shown in Fig. 10(b). This is because even at higher radial depth of cut, the layer of material removed by the cutting edge was very thin in the form of arc shaped uncut chip thickness. This arc of uncut chip is very thin at small feed rate and so can be removed in ductile mode. In this way, the length of the uncut chip arc, governed by radial depth of cut, was serving as length of cut for an equivalent orthogonal cutting process rendering the radial depth of cut fairly insensitive to the mode of cutting at that stage. However, this relation was not seen as entirely linear and independent. For same feed rate but at different radial depth of cuts, the brittle fracture in

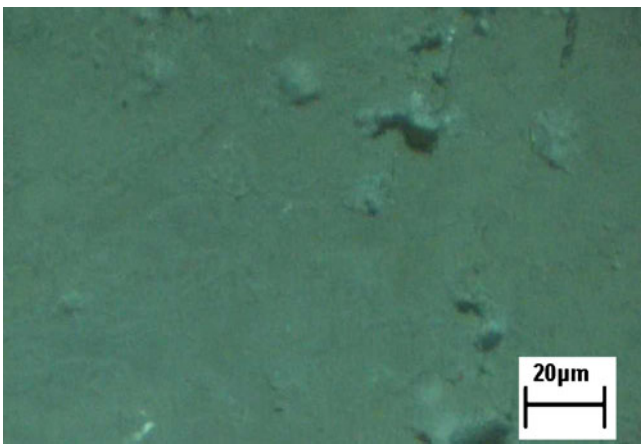

Fig. 9 Chips adhered on the machined surface

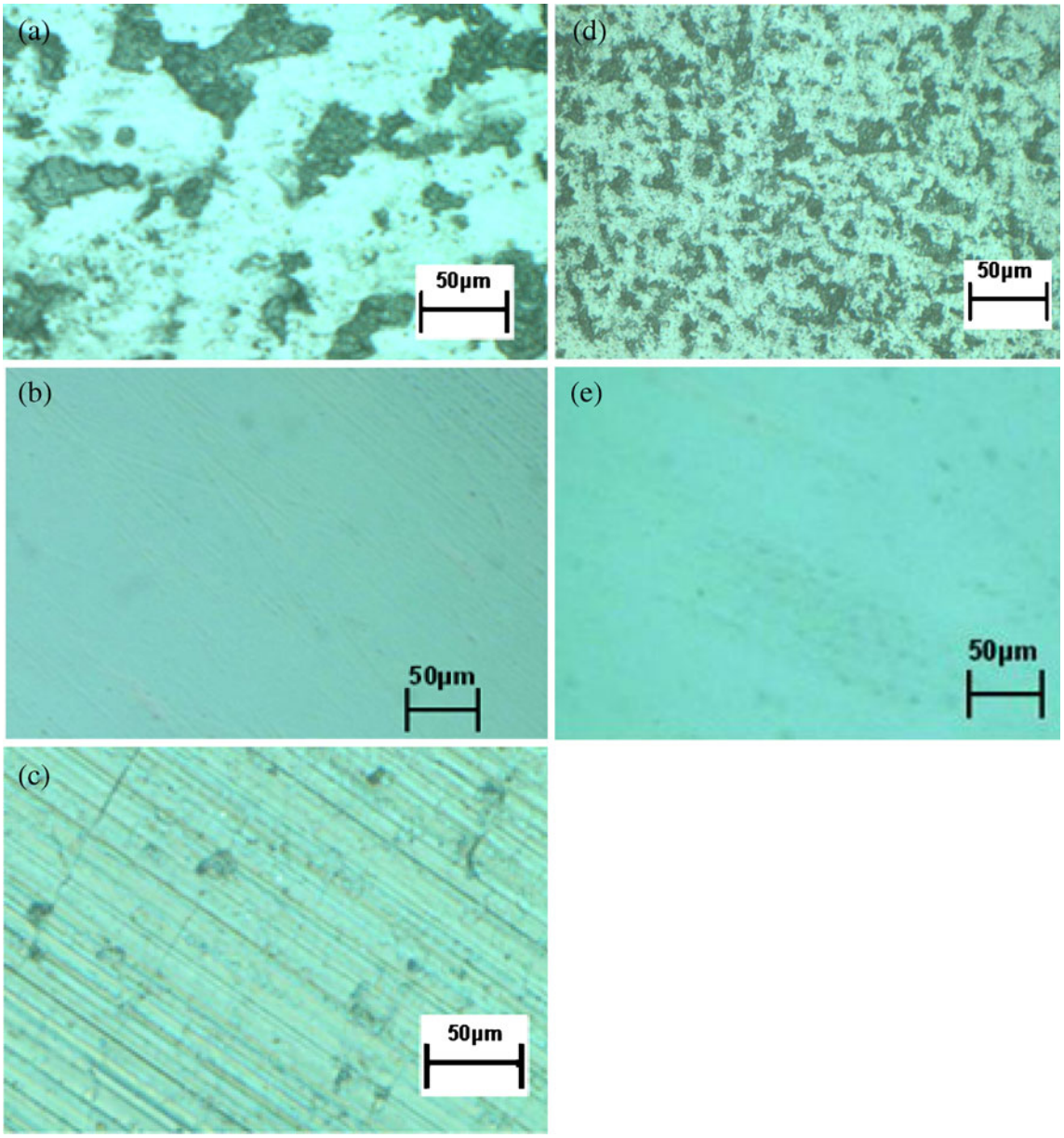

Fig. 10 Image of surfaces machined at **a** radial depth of cut=5 μm, feed rate=25 mm/min, **b** radial depth of cut=50 μm, feed rate=6 mm/min, **c** radial depth of cut=350 μm, feed rate=4 mm/min, **d** radial depth of cut=375 μm, feed rate=4 mm/min, and **e** radial depth of cut=275 μm, feed rate=4 mm/min

each case occurs at the same rotation angle of the cutter which means the fracture point is at the same distance from the final machined surface in this case. The observation of such machined surfaces, however, reveals that the surfaces machined with higher radial depth of cut were still having fracture marks as shown in Fig. 10c, d whereas the one machined at relatively smaller radial depth of cut was free of fracture as evident from Fig. 10e. This is perhaps because at higher radial depth of cut, the cutter-workpiece contact angle in the brittle zone becomes extended and therefore makes the energy required for crack propagation to be available in the brittle zone for longer duration of time. The extended fluctuations in cutting force due to repeated fractures allow the cracks originated from fracture point to propagate further towards the level of machined surface and eventually cross that level. So, the subsequent cut is not able to remove these fracture marks completely, and these marks appear on the final machined surface.

This effect is evident from cutting force signal at small and large radial depth of cuts with same feedrate as shown in Fig. 11. The cutting force signal at larger radial depth of cut given in Fig. 11a has steeper fluctuations for longer duration compared with that at smaller radial depth of cut as shown in Fig. 11b confirming that the brittle regime

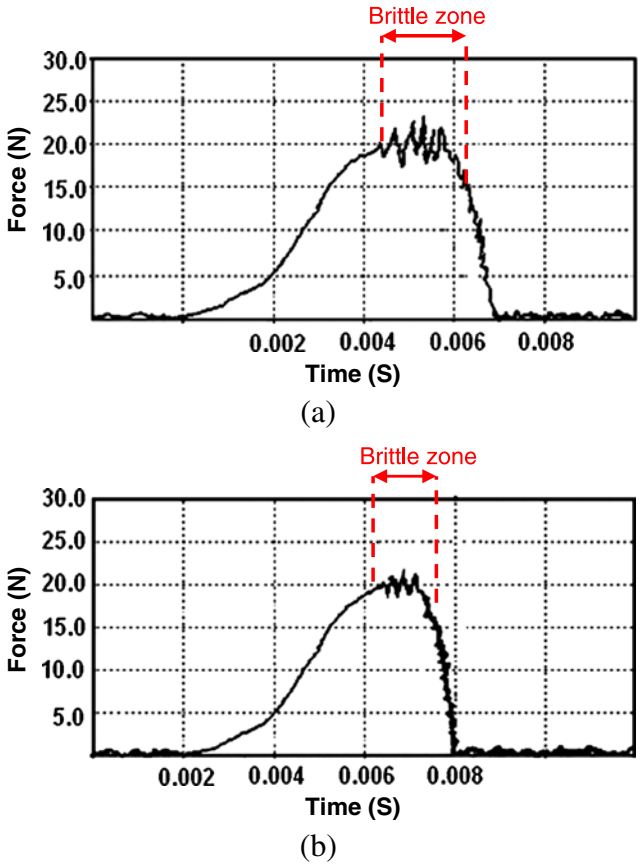

Fig. 11 Cutting force signal at **a** radial depth of cut=375 μm, feed rate=4 mm/min and **b** radial depth of cut=275 μm, feed rate=4 mm/min

occurred for comparatively longer duration. A further decrease in feed rate generated a fracture-free surface at high radial depth of cut by delaying the occurrence of brittle fracture.

The plot of thrust to cutting force ratio is given in Fig. 12. It is evident from the plot that the ratio decreases with the rotation angle of the cutter. As the rotation angle of the cutter increases, the uncut chip thickness also increases. This means the tangential component of the force has to increase correspondingly to remove or displace the material in the cutting direction which is tangent to the cutting point. Therefore, ratio of thrust to cutting force decreases with rotation angle. The ratio is more than unity at small undeformed chip thickness in ductile cutting conditions referring to the occurrence of plowing or rubbing at the beginning of the cut.

Based on the experimental results of this study, ductile and brittle regimes for side-milling are traced on a graph drawn between feed per edge and radial depth of cut shown in Fig. 13. The graph tends to become asymptotic towards the small values of radial depth of cut because of uncertainty in cutting mechanism due to plowing or rubbing effect at very small uncut chip thickness. In this zone, material may not be removed in every pass of the edge or tool because of minimum chip thickness limitation. To achieve effective cutting at such small value of radial depth of cut, very high feed per edge is desired to avoid minimum chip thickness effect. Such high values of feed per edge render the cutting action uncertain and unstable. On the other hand, it is evident from Table 3 and Fig. 13 that once the feed per edge reaches a value of 0.875 μm, the ductile cutting process seems to become insensitive to radial depth of cut and ductile machined surface is consistently obtained for higher values of radial depth of cut. Hence, this value of feed per edge is believed to be effective critical feed per edge. It is interpreted from this scenario that at very small values of feed per edge, the transitional uncut chip thickness occurs at an angle sufficiently far away from the final machined surface. Furthermore, the direction of crack propagation at that point is directed such that the cracks remain away from the machined surface at all times during cutting and are removed completely by the cutting action of the next edge. In this way, cutting mode becomes seemingly insensitive to the radial depth of cut for values larger than the corresponding value at minimum feed per edge used in this experiment. AFM analysis showed that best surface roughness achieved in this study was R_a=28.6 nm.

4.1 Tool wear

Two types of tool wear were observed. One wear was observed on flank face of the tool. This was mainly because of elastic recovery of the machined surface due to very small values of uncut chip thickness used in the cutting test. The elastic recovery of the machined surface, immediately after the cutting edge had passed the cutting zone, brings the newly machined surface in contact with flank face of

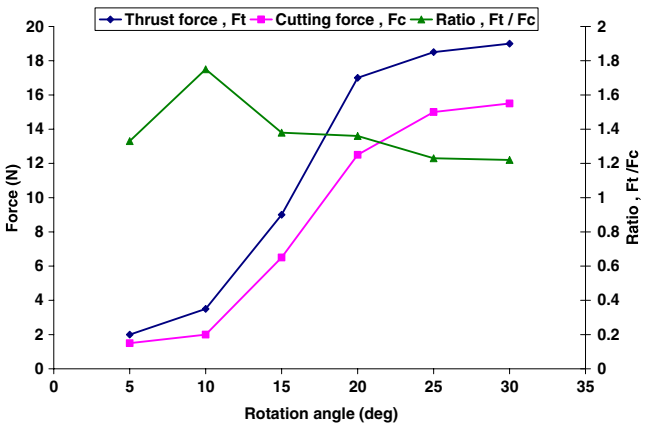

Fig. 12 Cutting forces vs. angle of rotation of cutter

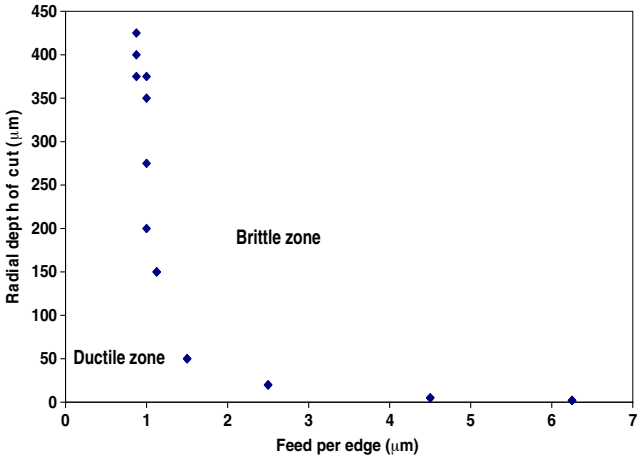

Fig. 13 Brittle-ductile transition boundary for side-milling

the tool causing this type of wear. The mechanism of this type of wear was abrasion dominant as shown in Fig. 14a. At relatively lower cutting speed and fine feeds used in this study, the heat generated in the cutting zone is not high enough to facilitate the diffusion or oxidation of the tool material. The wear on tool flank face is very consistent with the studies made on ductile-mode cutting by single edge cutting tool. The second type of wear formed grooves on the cutting edge resulted into gradual deformation of cutting edge after excessive cutting as evident from Fig. 14b. This type of wear affects the mode of cutting process significantly and causes the mode of machining to transit from ductile to brittle one. Due to this type of wear, the cutting edge does not remain sharp enough to maintain adequate hydrostatic compressive stress in the cutting zone leading to the opening of cracks.

Furthermore, scratches due to abrasion and wear marks on the edge cutting develop into the cracks that propagate under cyclic stress of the intermittent cutting action, eventually resulting into chipping of the tool as shown in Fig. 14c. No significant wear was observed on rake face of the tool due to occurrence of highly negative effective angle during ductile-mode cutting that prevents the chips to flow over the nominal rake face.

5 Conclusions

Microcutting of soda-lime glass was performed by end-milling process and following conclusions can be drawn from this study.

a. Within the controlled set of cutting conditions, fracture-free surface can be machined on glass by end-milling.
b. Feed per edge is the most dominant factor that governs the mode of machining in side-milling.
c. Below a certain value of feed per edge (0.875 μm), radial depth of cut becomes apparently insensitive to the mode of machining and fracture-free surface can be machined at high radial depth of cuts.
d. At very small radial depth of cut, ductile cutting can be achieved at higher feed per edge. This is important to prevent plowing and subsequent surface deterioration due to minimum chip thickness effect.
e. In milling process, it is not essential to achieve ductile cutting in the entire cutting zone. In fact, cutting conditions can be controlled in such a way that any fracture occurring somewhere in the cutting zone is prevented to reach from the final machined surface by the mechanics of cutting edge path.

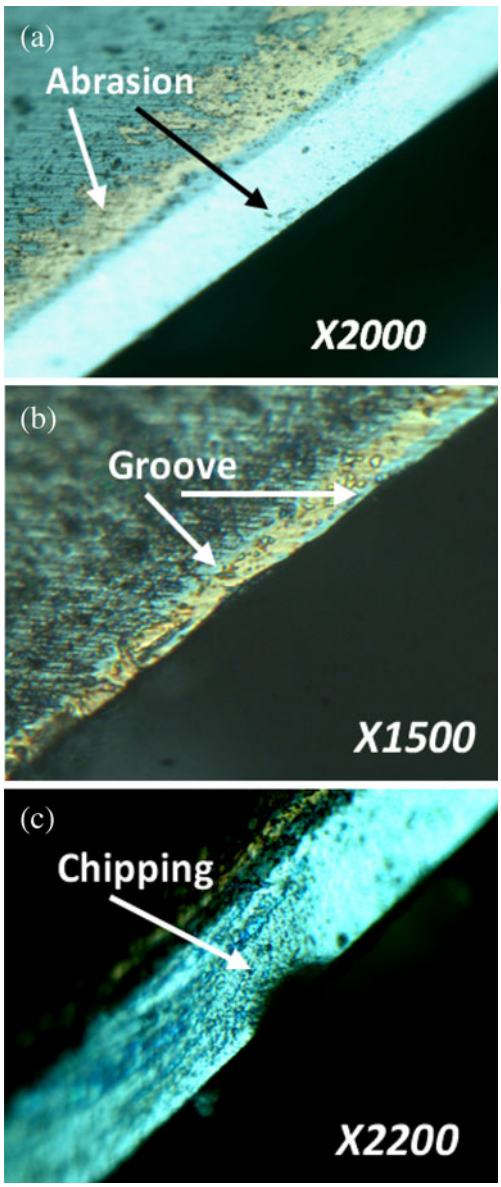

Fig. 14 Tools wear at **a** flank, **b** cutting edge, and **c** chipping of cutting edge

f. Wear was observed on the flank face and cutting edge of the tool.
g. Excessive wear causes the chipping of the cutting edge and mode of machining is transited from ductile to the brittle one.

Acknowledgement We are thankful to Dr. Tanveer Saleh and Mr. Vijay from MIKROTOOLS PTE LTD Singapore for providing assistance in conducting experiments.

References

1. Zhou M, Ngoi BKA, Yusoff MN, Wang XJ (2006) Tool wear and surface finish in diamond cutting of optical glass. J Mater Process Technol 174:29–33
2. Namba Y, Abe M (1993) Ultraprecision grinding of optical glasses to produce super-smooth surfaces. Ann CIRP 42(1):417–420
3. Foy K, ZhiWei TM, Huang Y (2009) Effect of tilt angle on cutting regime transition in glass micromilling. Int J Mach Tools Manuf 49:315–332
4. Jong de BHWS (1989) Glass. In: Ullmann's Encyclopedia of Industrial Chemistry, 5th edn. VCH Publishers, Weinheim, Germany, vol. A12. pp.365–432
5. Fang FZ, Chen LJ (2000) Ultra-precision cutting for ZKN7 glass. Ann ClRP 49(1):17–20
6. Liu K, Zuo D, Li XP, Rahman M (2009) Nanometric ductile cutting characteristics of silicon wafer using single crystal diamond tools. J Vacuum Sci Technol 27(3):1361–1366
7. Marshall DB, Lawn BR (1986) Indentation of brittle materials. In: Blau PJ, Lawn BR (eds) Microindentation techniques in materials science and engineering. American Society for testing and materials, Philadelphia, pp 26–46
8. Brehm R, Dun V, Teuunissen K, Haisma CG (1979) Transparent single-point turning of optical glass. J Precision Eng 1(3):207–213
9. Blackley WS, Scattergood RO (1991) Ductilc regime model for diamond turning of brittle materials. J Precision Eng 13(2):95–102
10. Gee AE, Spragg RC, Puttick KE, Rudman MR (1991) Single-point diamond form-finishing of glasses and other macroscopically brittle materials. Proc SPIE 1573:39–48
11. Moriwaki T, Shamato E, Inoue K (1992) Ultraprecision ductile cutting of glass by applying ultrasonic vibration. Ann CIRP 41:141–144
12. Komanduri R (1996) On material removal mechanisms in finishing of advance ceramics and glasses. Ann CIRP 45:509–513
13. Patten J, Gao W, Yasuto K (2005) Ductile regime nanomachining of single-crystal silicon carbide. Trans ASME 127:522–532
14. Yoshino M, Ogawa Y, Aravindan S (2005) Machining of hard-brittle materials by a single point tool under external hydrostatic pressure. J Manuf Sci Eng 127(4):837–845
15. Liu K, Li X, Liang SY, Liu XD (2004) Nanometer scale ductile mode cutting of soda- lime glass. Trans NAMRI/SME 32:39–45
16. Patten J, Gao W, Yasuto K (2005) Ductile regime nanomachining of single-crystal silicon carbide. J Manuf Sci Eng 127:522–532
17. Cai MB, Li XP, Rahman M (2007) Study of the mechanism of nanoscale ductile mode cutting of silicon using molecular dynamic simulation. Int J Mach Tools Manuf 47:75–80
18. Sreejith PS, Ngoi BKA (2001) Material removal mechanism in precision machining of new materials. Int J Mach Tools Manuf 41:1831–1843
19. Fang FZ, Zhang GX (2004) An experimental study of optical glass machining. Int J Adv Manuf Technol 23:155–160
20. Jared BH, Dow TA (1997) Chip dynamics in diamond turning. Proc ASPE 16:230–233
21. Shimada S, Ikawa N, Inamura T, Takezawa N, Ohmori H, Sata T (1995) Brittle-ductile transition phenomena in microindentation and micromachining. Ann CIRP 44(1):523–526
22. Lucca DA, Brinksmeier E, Goch G (1998) Process in assessing surface and subsurface integrity. Ann CIRP 47(12):669–694
23. Stavropoulos P, Salonitis A, Stournaras A, Pandremenos J, Paralikas J, Chryssolouris G (2007) Advances and challenges for tool condition monitoring in micro-milling. In: Proceeding of the IFAC workshop on manufacturing, management and control, Budapest, Hungry. pp. 157–162
24. Stavropoulos P, Salonitis A, Stournaras A, Pandremenos J, Paralikas J, Chryssolouris G (2007) Tool condition monitoring in micro-milling—a critical review. Advances in manufacturing technology XXI. In: Proceedings of the 5th international conference on manufacturing research, Leicester, UK. pp. 324–328
25. Stavropoulos P, Stournaras A, Chryssolouris G (2009) On the design of a monitoring system for desktop micromilling machines. Int J Nanomanuf 3(1/2):29–39
26. Takeuchi Y, Sawada K, Sata T (1996) Ultraprecision 3D micro-machining of glass. Ann CIRP 45(1):401–404
27. Matsumura T, Ono T (2005) Glass machining with ball end mill. Trans NAMRI/SME 33:319–326
28. Matsumura T, Hiramatsu T, Shirakashi T, Muramatsu T (2005) A study on cutting force in the milling process of glass. J Manuf Processes 7(2):102–108
29. Matsumura T, Ono T (2008) Cutting process of glass with inclined ball end mill. J Mater Process Technol 200:356–363
30. Ono T, Takashi M (2008) Influence of tool inclination on brittle fracture in glass cutting with ball end mills. Int J Mater Process Technol 202:61–69
31. Kim C-J, Mayor JR, Ni J (2004) A static model of chip formation in microscale milling. Trans ASME J Manuf Sci Eng 126:710–718
32. Chae J, Park SS, Freiheit T (2006) Investigation of micro-cutting operations. Int J Mach Tools Manuf 46:313–332
33. Basuray PK, Misra BK, Lal GK (1977) Transition from ploughing to cutting during machining with blunt tools. Wear 43:341–349
34. Chiu WC, Endres WJ, Thouless MD (2000) An experimental study of orthogonal machining of glass. Mach Sci Technol 4 (2):253–275
35. Chiu WC, Endres WJ, Thouless MD (2001) An analysis of surface cracking during orthogonal machining of glass. Mach Sci Technol 5(2):195–215
36. Sreejith P (2005) Machining force studies on ductile machining of silicon nitride. J Mater Process Technol 169(3):414–417
37. Rusnaldy Ko TJ, Kim HS (2007) An experimental study on microcutting of silicon using a micromilling machine. Int J Adv Manuf Technol 39(1–2):85–91